Enhancement of Cobalt Catalyst performance and Stability in Fischer-Tropsch Synthesis Using Graphene Nanosheets as Catalyst Support

Somayeh Taghavi[a], Alireza Asghari[a*], Ahmad Tavasoli[b]

[a]Department of Chemistry, Semnan University, Semnan, Iran

[b]School of chemistry, College of Science, University of Tehran, Tehran, Iran

A b s t r a c t

Graphene nano sheets (GNS) supported cobalt catalyst, is introduced for Fischer-Tropsch synthesis (FTS). The catalyst was prepared using wet impregnation method with cobalt loading of 15.0 wt%. The physico-chemical properties of the catalyst is investigated by TPR, TPD, BET, XRD, TEM and H_2 chemisorption methods. The performance of the catalyst was assessed in a fixed bed micro-reactor at 220^oC, 18 bars and H_2/CO ratio of 2. The results were compared with those of Co/ γ-alumina. Using GNS as cobalt catalyst support decreased the average cobalt particles size from 16 to 9 nm, increased cobalt dispersion from 6 to 21% and improved the catalyst reducibility by a factor of 2.25. The activity of Co/GNS catalyst in FTS enhanced in comparison with that obtained for $Co/\gamma-Al_2O_3$. The products selectivity showed a slight shift to lower molecular weight hydrocarbons. Using GNS as catalyst support increased the catalyst lifetime.

Keywords Fischer-Tropsch synthesis, Graphene nano sheets, Al_2O_3, performance, Stability

1. Introduction

Fischer-Tropsch synthesis produces hydrocarbons from syngas, which is a mixture of carbon monoxide and hydrogen. Depending on catalyst, reactor type and reaction conditions, FT synthesis could produce a wide range of hydrocarbons such as light hydrocarbons, gasoline, diesel fuel and wax [1-3]. One important focusin development of this process is improving the catalyst activity by increasing the number of surface active Co sites which are stable under the reaction conditions [4]. Previous studies showed that a drawback of the FTS commercial catalysts (cobalt dispersed on porous carriers such as SiO_2, Al_2O_3 and TiO_2) is their support reactivity toward cobalt, which during preparation or catalysis results in the formation of mixed compounds that are reducible only at very high reduction temperatures [5]. Formation of these compounds depends on the nature of support and interactions of support with cobalt [6]. Furthermore, interactions cobalt with support may also depend on the amount of metal loading[7].

In recent years, some novel carbon materials, such as carbon nano fibers (CNFs), carbon nanotubes (CNTs) and graphene nano sheets (GNS), have become the most interesting catalyst supports [8]. CNFs and CNTs have been used as cobalt FTS catalyst supports[9]. Compared to CNFs and CNTs, GNS has better structural, mechanical and chemical stability and improved

electronic properties [10,11]. GNS with its two-dimensional sheet of sp^2-hybridized carbon, provides a high specific surface area and influences the dispersion of the metal clusters and also electronically modifies the active metal sites.

In this work, the catalytic properties of Co/GNS catalyst prepared by the sequential aqueous incipient wetness impregnation method are presented. The cobalt loading was 15 wt.%. The physico-chemical characteristics and catalytic performance of the catalyst is evaluated and the results are compared by commercial γ-alumina supported cobalt catalyst with the same cobalt loading.

2. Experimental procedure

2.1. Catalyst preparation

RIPI-GNS (Purity > 99.5%) was used as support material for preparation of cobalt catalysts. GNS supported catalyst was prepared with cobalt loadings of 15 wt.%. Prior to catalyst preparation, support was refluxed with 30% HNO_3 at 120°C overnight, washed with distilled water several times and dried at 120°C for 6 h. This approach creates oxygen containing OH functional groups on both the edges and basal plane of GNS, which can be used as chemically active anchoring sites for metal particles. The catalyst was prepared using an aqueous solution of cobalt nitrate. The sequential impregnation method was used to add Co $(NO_3)_2 \cdot 6H_2O$ (99.0%, Merck) to the support. After impregnation, catalyst was dried at 120°C and then were calcined at 350°C for 4 h with a heating rate of 1°C/min. Also one γ-alumina supported (Conndea Vista Catalox B γ-alumina) catalyst with cobalt loading of 15 wt.% was prepared just for comparison purposes. This catalyst was dried at 120°C and calcined at 350°C for 3 h with a heating rate of 1°C /min. The catalysts nomenclature and compositions are listed in Table 1.

2.2 Catalyst characterization

Weight percentages of Co metal in the catalysts were measured by inductively coupled plasma (ICP) method using a Varian VISTA-MPX instrument. Catalysts were suspended in methanol using an ultrasonic bath and dropped onto a carbon coated copper grid to take the TEM images of the samples using a Philips CM20 (100 kV) transmission electron microscope equipped with a NARON energy-dispersive spectrometer with a germanium detector. BET surface area measurements were carried out using an ASAP-2010 system from Micromeritics. In each trial, a weight of approximately 0.25 g of sample was degassed at 200°C for 4h under 50 mTorr vacuum and the BET area, pore volume, and average pore radius were determined.

A Philips analytical X-ray diffractometer (XPert MPD) with monochromatized Cu/Kα was used to record the X-ray diffraction patterns (XRD) of the catalysts. Co_3O_4 crystallite size was estimated based on the Debye–Scherrer equation [12].

H_2-TPR was conducted on catalysts using Micrometrics TPD–TPR 2900 system equipped with a thermal conductivity detector (TCD). First traces of water and gases were removed from the catalysts by purging with helium at 140°C. Then, after cooling to 40°C, TPR of each sample was performed using 5% H_2 in Ar stream with flow rate of 40 ml/min at atmospheric pressure at a linearly programmed heating (10°C/min) up to 850°C.

The amounts of chemisorbed hydrogen on the catalysts were measured using the Micromeritics TPD-TPR 290 system. 0.25 g of the calcined catalyst was reduced under hydrogen at 400°C for 20 h and then cooled to 50°C under hydrogen. Then the flow of hydrogen was switched to argon at the same temperature, which lasted for about 30 min in order to remove the physis or bed hydrogen. Afterwards, the temperature programmed desorption (TPD) of the samples was obtained by increasing the temperature of the samples, with a ramp rate of 20°C/min, to 400°C under the argon flow. After TPD of hydrogen, the sample was re-oxidized at 400°C by pulses of 10% oxygen in helium to determine the extent of reduction. It is to note that during reoxidation of the catalysts, no CO_2 peak is observed indicating that GNS has not reacted with oxygen. The data were used to determine the cobalt dispersion, percentage reduction and cobalt average crystallite size. The dispersion, percentage reduction

and particle diameter are calculated by the following formula [13].

$$\%Dispersion$$
$$= \frac{number\ of\ Co^0 atoms\ on\ surface}{number\ of\ Co\ atoms\ in\ sample}$$
$$\times 100 \qquad (Equation\ 1)$$

$$Fraction\ reduced$$
$$= \frac{O_2\ Uptake\ \times \frac{2}{3} \times atomic\ weight}{Percentage\ metal}$$
$$(Equation\ 2)$$

$$Diameter(nm)$$
$$= \frac{6000}{Density\ \times\ maximum\ area \times dispersion}$$
$$(Equation\ 3)$$

2.3. Reaction setup and experimental outline

The catalysts were evaluated in terms of their Fischer–Tropsch synthesis (FTS) activity (g HC produced/g cat/min) and selectivity (the percentage of the converted CO that appears as a hydrocarbon product) in a tubular fixed-bed micro-reactor. Typically, 0.7 g of the catalyst diluted with 2.1 g of SiC to eliminate the temperature gradient and charged into the reactor. The reactor temperature was maintained constant ($\pm 1^{\circ}$C) by a PID temperature controller. Brooks 5850 mass flow controllers were used to add H_2 and CO at the desired flow rates and the mixed gases entered through the top of the reactor. The catalysts were reduced in H_2 flow at 400°C, with a heating rate of 1°C /min for 16 hours. Following activation, syngas (H_2/CO = 2) was injected with a flow rate of 45 ml/min. The temperature and pressure were maintained at 220° C and 1.8 MPa, respectively. Products were continuously removed from the vapor and passed through two traps, one maintained at 100°C (hot trap) and the other at 0°C (cold trap). The uncondensed vapor stream was reduced to atmospheric pressure through a pressure letdown valve. The outlet flow was measured with a bubble-meter and it's composition quantified using an on-line GC. The

contents of hot and cold traps were removed every 24 h, the hydrocarbon and water fractions were separated, and then analyzed by a Varian 3800 gas chromatograph equipped with a capillary column and a flame ionization detector.

3. Results and discussion

3.1. Supports and catalysts characterization

Results of surface area measurement and textural properties of the supports and catalysts are listed in Table 1. GNS presents an ideal two-dimensional material composed of layers of atoms organized in a hexagonal lattice and connected by sp^2 in-plane carbon−carbon bonds. This structure exhibits a high specific surface area. As shown, the decrease of BET surface area and pore volume is higher in the case of the catalyst supported on GNS. Loading of 15wt.% cobalt on γ-Al_2O_3 decreased the BET surface area from 270 to 214 m^2/g (indicating 20.7% decrease), However the same loading of cobalt on GNS, decreased the BET surface area for 373 to 255 m^2/g (indicating 31.6% decrease).

Table1: BET surface area and XRD results

Support / Catalyst	Co (wt.%)	BET (m^2/g)	Pore Volume (Single point) (cm^3/g)	Average Pore Radius (nm)	d_{Co3O4} (nm) determined by XRD
γ-Al_2O_3	-	270	0.639	4.72	-
GNS	-	373	1.45	0.78	-
15Co/GNS	14.88	255	0.63	0.62	12.0
15Co/ γ-Al_2O_3	14.84	214	0.439	4.26	14.7

Figures 1a shows the TEM image of the 15wt.% Co/GNS catalyst after calcination, at 350°C. The dark spots represent the cobalt oxides which are attached to the support surface. The TEM image show remarkably uniform cobalt nano particles that are well dispersed on the GNS surface. As shown, the well-dispersed metal nanoparticles with an average size of 5-11 nm are formed. Figure 1b shows the TEM image of the 15wt.% Co/γ-Al_2O_3 catalyst after calcination 350°C. The TEM micrograph of the calcined 15wt.% Co/γ-Al_2O_3 catalyst reveals that the catalyst particles are dispersed on the

surface of alumina. Dark spots represent the cobalt oxides which are attached to the surface of alumina. The cobalt oxide particles inside the pores of alumina are moderately uniform and the most abundant ones have sizes in the range of 5-15 nm.
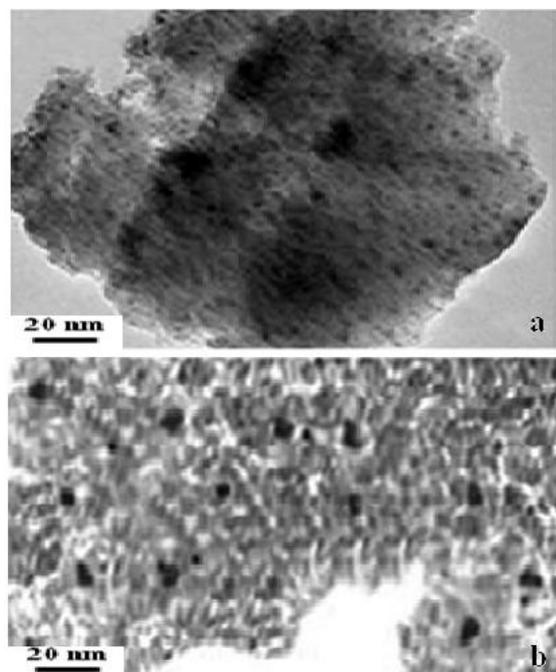

Figure 1. TEM images of the 15wt.% Co/GNS and 15wt.% Co/γ-Al$_2$O$_3$

patterns of the supports and catalysts are shown in Figure 2. In the XRD of Co/Al$_2$O$_3$ catalyst peaks at 46.1 and 66.5° correspond to Al$_2$O$_3$, while the other peaks, except that at 49° peak, which is attributed to the cobalt aluminates [14], relate to the different crystal planes of Co$_3$O$_4$. In the pattern of GNS supported catalyst, the peaks at 25 and 43° correspond to GNS [15]. The other peaks with 2θ values of 31.3, 36.8, 45.8, 59.4, and 65.3 could be attributed to the Co$_3$O$_4$ spinel phase in the catalyst [16]. In contrast to the 49° peak in the spectrum of Co/Al$_2$O$_3$ catalyst, which is attributed to the cobalt aluminates, in the XRD patterns of GNS supported catalyst no peak was observed indicating formation of cobalt support compounds. The peak at 36.8° is the most intense peak of Co$_3$O$_4$ in XRD pattern of all catalysts. Table 1 shows the average Co$_3$O$_4$ crystallite sizes calculated from XRD spectrum and Scherrer equation at

2θ value of 36.8°[17]. Comparing the average Co$_3$O$_4$ crystallite size for 15wt.% Co/GNS and 15wt.% Co/γ-Al$_2$O$_3$ catalysts, reveals that the average Co$_3$O$_4$ crystallite size for GNS supported catalyst is smaller than that of γ-Al$_2$O$_3$ supported catalyst. Higher surface area of GNS support will lead to better distribution of particles, which in turn leads to lower cobalt cluster sizes.
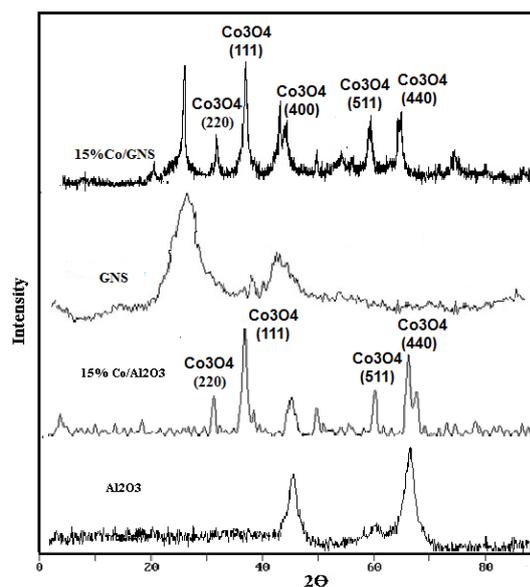

Figure 2: XRD patterns of the calcined Co/GNS and Co/Al$_2$O$_3$ catalysts

The TPR spectra of the calcined catalysts are shown in Figure 3. In this Figure, in the TPR profile of alumina supported catalyst the first peak is typically assigned to the reduction of Co$_3$O$_4$ to CoO, although a fraction of the peak likely comprises the reduction of the larger, bulk-like CoO species to Co°. The second peak, with a broad shoulder is mainly assigned to the second step reduction, which is mainly reduction of CoO to Co°. This peak also includes the reduction of cobalt species that interact with the support, which extends the TPR spectra to higher temperatures. As shown in this Figure, a reduction feature for Co/Al$_2$O$_3$ catalyst observed in the temperature range of 700–950°C, with a maximum centered at about 804°C. Such a high reduction temperature might be assigned to the reduction of cobalt aluminates species formed by reaction of highly

dispersed CoO with the alumina. In fact, cobalt aluminates were shown to reduce at temperatures well above 800ºC, while bulk Co_3O_4 became completely reduced at temperatures below 500ºC [18]. All these features suggest that part of the cobalt in the alumina supported cobalt catalysts strongly interacts with the support, as also evidenced from XRD patterns. Figure 3 also shows the TPR of the GNS supported cobalt catalyst. In the case of Co/GNS sample, the first and second reduction peaks were found at 368ºC and 523ºC .As shown, the first and second reduction peaks significantly shifted to lower temperatures. The reduction at lower temperatures shows that the reducibility of Co_3O_4 particles is easier in the case of the catalyst supported on GNS. This could be attributed to spillover of H_2 from the functional groups. According to H_2 spillover phenomena on GNS, where H atoms tend to group into compact clusters, possible nucleation centers can be lattice defects. In that case it lowers the reaction H_2 dissociation transition state as a catalyst and reduces the nucleation barrier so the defects present on the surface of the GNS facilitate the reduction by accelerating H_2 spillover. Typically, the ratio of the hydrogen consumed in the first reduction step to that consumed in the second reduction step is about 1:3. The amount of hydrogen consumed in the first reduction peak was lower than the expected amount; this could only be ascribed to the reduction of nitrates rather than the reduction of Co_3O_4.
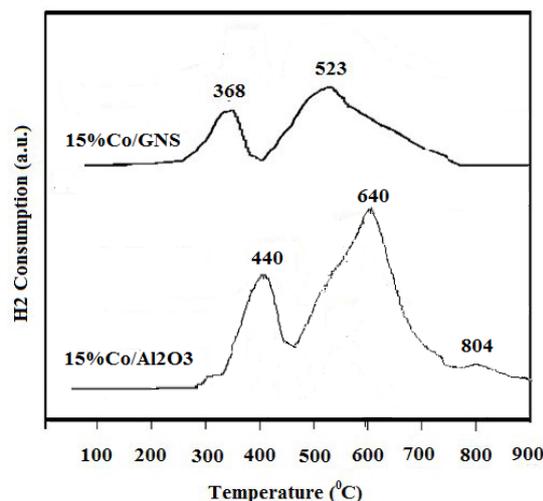

Figure 3. TPR patterns of the calcined Co/GNS and Co/Al₂O₃ catalysts from 40 to 850ºC

The results of hydrogen TPD and oxygen titrations for all the catalysts are presented on Table 2. Comparing the results of 15wt.% Co/GNS and 15wt.% Co/γ-Al₂O₃ catalysts, the hydrogen uptake increased by a factor of 3.2 by using GNS as cobalt catalyst support. In agreement with the results of TPR, results in this Table indicate that a remarkable improvement in the percentage reduction is obtained by switching to GNS support with the same loading (i.e. increased by a factor of 2.29). While the dispersion of the cobalt crystallites calculated based on the total amount of cobalt increased significantly, the average cobalt particle size decreased which is due to higher surface area of GNS, lower degree of agglomeration of the cobalt crystallites and lower interaction of cobalt with support in GNS supported catalyst. These results are in agreement with the results of XRD and TEM. Larger dispersion and lower cobalt cluster size will increase greatly the number of sites available for FT reaction in GNS supported catalysts with the same loading.

Table 2: Crystallite sizes of unreduced cobalt particles determined by H_2 temperatures programmed desorption and pulse reoxidation of catalysts.

Catalyst	µ mole H_2 desorption /g cat.	µ mole O_2 Consumption /g cat.	%Red.	%Dispersion	dp (nm
Co/GNS	246	1382	72	21.6	9
Co/Al₂O₃	77	601	32.00	6.02	16.6

3.2. Activity and products selectivity and catalyst stability results

The results of Fischer-Tropsch synthesis rate (g HC produced/ g cat/ h), and the percentage CO conversion at 220ºC, 1.8 MPa, and a H_2/CO ratio of 2 for Co/Al₂O₃ and Co/GNS catalysts are given in Table 3. Data on this table reveals that cobalt catalyst supported on GNS significantly enhances the CO conversion and FT synthesis rate. CO conversion and the FTS rate show an increase of about 80% in accordance with hydrogen uptake, percentage reduction and percentage dispersion (Table 2). Table 3 reveals that the FTS rate and CO conversion are strongly dependent and proportional to the number of surface reduced active cobalt sites. It is to note that the rate of water gas shift reaction or CO_2 formation rate was negligible for both catalysts.

The change in CO conversion and FT synthesis rate could be possibly explained by perusing the structural and electronic properties of Co/GNS catalyst. It has been shown that the Co atom serves as a donor to supply electrons, which are partly transferred to saturate the electronic states of carbon atoms in the GNS   and   the   rest   transferred to bind the gas adsorption. CO molecules as acceptors gain electrons from the Co/GNS substrates. Gaining more electrons will result more stable adsorptions. However, the enhanced electron transfer from carbon atoms to the adsorbed H_2 is the main drive for H_2 dissociation and this could increase the density of reactants , and hence create a locally higher concentration which will favor CO hydrogenation [19]. The presence of the OH groups on GNS and the more surface reduced Co atoms, which

are present on Co/GNS catalyst accelerates charge transfers [20].

Table 3: Activity Products selectivity of 15wt.% Co/GNS and 15wt.% Co/γ-Al₂O₃

Catalyst	% CO Conversion	C_5^+	CH_4	Rate (gr CH/gr cat./hr)
Co/GNS	70.6	86.8	12.3	0.325
Co/Al₂O₃	39.9	88.2	11.3	0.18

Table 3 and figure 4 also shows the effects of support on the selectivity of Fischer-Tropsch synthesis products. Comparing the product distributions for Co/Al₂O₃ and Co/GNS catalysts, clearly demonstrates that, unlike to the significant improvement in the CO conversion and FTS rate, product distribution shows a slight shift to lower molecular weight hydrocarbons in GNS supported cobalt catalyst. C_5^+ selectivity is decreased by 1.5% , CH_4 selectivity is increased by 8.8% for GNS supported catalyst. It is believed that in FTS the larger cobalt particles are more selective to larger hydrocarbons and the smaller particles are selective for methane and light gases. It seems that for Co/Al₂O₃ catalyst, which has larger cobalt clusters (Table 2), the steric hindrance for dissociative adsorption of CO and -CH_2- monomer and addition of this monomer to the growing chain is less. On the other hand, chain propagation and growth probability at the surface of the large clusters of Co/Al₂O₃ catalyst is more than that of the smaller clusters of Co/GNS catalyst. The increase in methane and light gaseous products and the decline of C_5^+ hydrocarbons for GNS supported catalyst is not significant comparing to the large improvement of FTS rate of 80%. In industrial scale, increasing the methane and light gaseous products selectivity will slightly increase the amount of recycling to syngas production unit resulting in larger syngas and FT reactors and higher capital cost of the plant. However, in the case of the GNS supported cobalt catalyst 80% enhancement of reaction rate will decreases the size of FT reactor and hence the capital cost, significantly. Process   optimization   and   overall   economical calculations are necessary to determine the effects of these variables on the capital cost of an industrial plant.

In industrial scale, GNS supported FT synthesis catalyst with high productivity will decrease reactor volume requirements. Since FT reaction is not a fast reaction, industrial scale FT reactors are very big reactors. Therefore, using GNS supported cobalt catalyst can decrease the industrial scale reactors volume and improve process economics significantly. On the other hand, in order to increase the reducibility and activity of the conventional γ-Al_2O_3 supported cobalt catalysts, ruthenium and rhenium are used as cobalt catalyst promoters. Indeed, these promoters can increase the reducibility and activity of the conventional metal oxide supported cobalt catalysts, the application of ruthenium and rhenium as cobalt catalyst promoters in FTS is restricted due to their high price. Excellent reducibility and high activity of GNS supported cobalt catalysts makes it a suitable candidate for industrial FT processes and eliminate the need for such costly promoters.
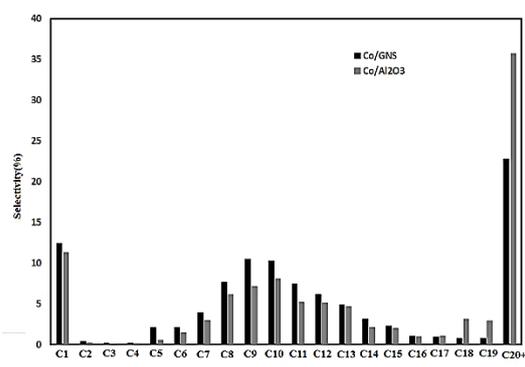

Figure 4. hydrocarbon product distributions for Co/Al_2O_3 and Co/GNS catalysts (T = 220ºC, P = 1.8MPa and H_2/CO = 2).

Figure 5 shows the variations of CO conversion with the time on stream (TOS) for 15wt.% Co/GNS and 15wt.% Co/γ-Al_2O_3 catalysts. As shown, for 15wt.% Co/GNS catalyst, 240 hrs continues FT synthesis decreased the % CO conversion from 70.6 to 67.3% (i.e. 4.6% decrease in catalyst activity). At the same time for Co/γ-Al_2O_3 catalyst the % CO conversion decreased from 39.9 to 32% (i.e. 19.8% decrease in catalyst activity). It has been shown that water produced during the FT synthesis is the main reason for catalyst deactivation [21]. Recent experimental works indicate that the contact angle of water on

GNS is significantly higher than that of other supports. This suggests that GNS could be one of the most hydrophobic surfaces with very weak interaction with the water molecules [22]. This will decrease the water induced oxidation of cobalt, formation of compounds between cobalt and support and the oxidation-reduction cycles on the catalyst surface which led to the sintering or cluster growth.
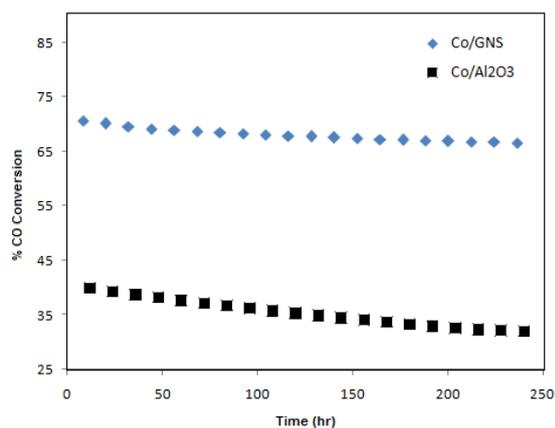

Figure 5. Variations of %CO conversion with time-on-stream for Co/GNS and Co/γ-Al_2O_3 catalysts

4. Conclusion

GNS was used as cobalt FTS catalyst support. Using GNS as cobalt catalyst support decreased the average cobalt particles size, increased cobalt dispersion and improved the catalyst reducibility. From a catalytic activity standpoint, the performance of catalyst in FTS considerably enhanced in comparison with that obtained from cobalt on γ-Al_2O_3. The products selectivity showed a slight shift to lower molecular weight hydrocarbons. GNS increased the catalyst stability. Using GNS as catalyst support increased the catalyst lifetime.

References

[1] Adesina AA. Hydrocarbon synthesis via Fischer-Tropsch reaction: travails and triumphs. Applied Catalysis A: General. 1996;138(2):345-67.

[2] Keypour H, Noroozi M. Hydrogenation of benzene in gasoline fuel over nanoparticles (Ni, Pt, Pd, Ru and Rh) supported fullerene: Comparison study. Journal of Applied Chemistry. 2016;10 (37):31-42.

[3] Mohamadkhani B, Haghighi M, Aghaei E. Preparation and evaluation of nanostructured composite SAPO-34 (90%)/HZSM-5 (10%) catalyst used in conversion of methanol to ethylene and propylene. Journal of Applied Chemistry. 2016;11(39):65-84.

[4] Dry ME. The Fischer–Tropsch process: 1950–2000. Catalysis today. 2002;71(3):227-41.

[5] Li T, Wang H, Yang Y, Xiang H, Li Y. Study on an iron–nickel bimetallic Fischer–Tropsch synthesis catalyst. Fuel Processing Technology. 2014;118:117-24.

[6] Medina C, García R, Reyes P, Fierro J, Escalona N. Fischer Tropsch synthesis from a simulated biosyngas feed over Co (x)/SiO 2 catalysts: Effect of Co-loading. Applied Catalysis A: General. 2010;373(1):71-5.

[7] Feyzi M, Irandoust M, Mirzaei AA. Effects of promoters and calcination conditions on the catalytic performance of iron–manganese catalysts for Fischer–Tropsch synthesis. Fuel Processing Technology. 2011;92(5):1136-43.

[8] Panpranot J, Kaewkun S, Praserthdam P, Goodwin Jr JG. Effect of cobalt precursors on the dispersion of cobalt on MCM-41. Catalysis letters. 2003;91(1-2):95-102.

[9] Li J, Cheng X, Zhang C, Yang Y, Li Y. Effects of alkali on iron-based catalysts for Fischer-Tropsch synthesis: CO chemisorptions study. Journal of Molecular Catalysis A: Chemical. 2015;396:174-80.

[10] Rytter E, Holmen A. Deactivation and Regeneration of Commercial Type Fischer-Tropsch Co-Catalysts—A Mini-Review. Catalysts. 2015;5(2):478-99.

[11] Dindari M, Momeni M, Goodarzi Rad M. Electrochemical fabrication of Polyaniline-Graphene Quantum films containing gold nanoparticles deposited on titanium electrode for electro-oxidation of ascorbic acid. Journal of Applied Chemistry. 2015;10 (36):97-106.

[12] Asami K, Iwasa A, Igarashi N, Takemiya S, Yamamoto K, Fujimoto K. Fischer–Tropsch synthesis over precipitated iron catalysts supported on carbon. Catalysis today. 2013;215:80-5.

[13] Machado BF, Serp P. Graphene-based materials for catalysis. Catalysis Science & Technology. 2012;2(1):54-75.

[14] Tavasoli A. Catalyst composition and its distribution effects on the enhancement of activity, selectivity and suppression of deactivation rate of FTS cobalt catalysts: Ph. D. Thesis, University of Tehran: Tehran, Iran; 2005.

[15] Jacobs G, Patterson PM, Das TK, Luo M, Davis BH. Fischer–Tropsch synthesis: effect of water on Co/Al 2 O 3 catalysts and XAFS characterization of reoxidation phenomena. Applied Catalysis A: General. 2004;270(1):65-76.

[16] Tavasoli A, Mortazavi Y, Khodadadi A, Sadagiani K. Effects of different loadings of Ru and Re on physico-chemical properties and performance of 15% Co/Al2O3 FTS catalysts. Iranian Journal of Chemistry and. 2005.

[17] Tavasoli A, Trépanier M, Dalai AK, Abatzoglou N. Effects of confinement in carbon

nanotubes on the activity, selectivity, and lifetime of Fischer− Tropsch Co/carbon nanotube catalysts. Journal of Chemical & Engineering Data. 2010;55(8):2757-63.

[18] Naeimi H, Mohajeri A, Moradi L, Rashidi AM. Efficient and facile one pot carboxylation of multiwalled carbon nanotubes by using oxidation with ozone under mild conditions. Applied Surface Science. 2009;256(3):631-5.

[19] Serp P, Corrias M, Kalck P. Carbon nanotubes and nanofibers in catalysis. Applied Catalysis A: General. 2003;253(2):337-58.

[20] Chen W, Fan Z, Pan X, Bao X. Effect of confinement in carbon nanotubes on the activity of Fischer− Tropsch iron catalyst. Journal of the American Chemical Society. 2008;130(29):9414-9.

[21] Trépanier M, Dalai AK, Abatzoglou N. Synthesis of CNT-supported cobalt nanoparticle catalysts using a microemulsion technique: role of nanoparticle size on reducibility, activity and selectivity in Fischer–Tropsch reactions. Applied Catalysis A: General. 2010;374(1):79-86.

[22] Tavasoli A, Karimi S, Taghavi S, Zolfaghari Z, Amirfirouzkouhi H. Comparing the deactivation behaviour of Co/CNT and Co/γ-Al 2 O 3 nano catalysts in Fischer-Tropsch synthesis. Journal of Natural Gas Chemistry. 2012;21(5):605-13.